
ESSEN: Improving Evolution State Estimation for Temporal Networks using Von Neumann Entropy

Anonymous Author(s)

Affiliation

Address

email

Abstract

1 Temporal networks are widely used as abstract graph representations for real-world
2 dynamic systems. Indeed, recognizing the network evolution states is crucial in
3 understanding and analyzing temporal networks. For instance, social networks
4 will generate the clustering and formation of tightly-knit groups or communities
5 over time, relying on the triadic closure theory. However, the existing methods
6 often struggle to account for the time-varying nature of these network structures,
7 hindering their performance when applied to networks with complex evolving
8 states. To mitigate this problem, we propose a novel framework called ESSEN, an
9 Evolution StateS awareE Network, to measure temporal network evolution using
10 von Neumann entropy and thermodynamic temperature difference. The developed
11 framework utilizes the von Neumann entropy aware attention mechanism and
12 network evolution state contrastive learning in the graph encoding. In addition,
13 it employs a unique decoder Mixture of Thermodynamic Experts (MoTE) for
14 decoding. ESSEN extracts local and global network evolution information using
15 thermodynamic features and adaptively recognizes the network evolution states.
16 Moreover, the proposed method is evaluated on link prediction tasks with transduc-
17 tive settings and inductive settings, with the corresponding results demonstrating
18 its effectiveness compared to various state-of-the-art baselines ¹.

19 1 Introduction

20 In recent years, graph representation learning has demonstrated excellent performance in a variety
21 of static graphs [7; 14][28; 18]. Indeed, the success of static graph representation learning has led
22 to a growing interest in continuous-time dynamic graph representation learning. Temporal network
23 representation learning has emerged as an active research area focusing on learning low-dimensional
24 representations that capture their topological and temporal properties. However, in many temporal
25 networks, which are naturally generated in real-world systems, such as social networks[12] and
26 citation networks, learning effective representations is still a difficult task. The evolving nature of
27 these networks poses a significant challenge for network analysis and modeling, as the relationships
28 between nodes and their properties evolve. The existing methods often struggle to account for
29 the time-varying nature of these network structures, hindering their performance when applied to
30 networks with complex evolving states. However, capturing the evolving states of temporal networks
31 suffers from the following challenges: (1) Temporal networks have different types of evolving
32 states, such as periodic, linear, or non-linear changes in their structure over time. Moreover, the
33 evolving patterns can be changed in the network’s different evolving stages. As illustrated in Fig.1,
34 the evolution speed varies at different times in both datasets. The MathOverflow network evolves
35 rapidly and has obvious central nodes, which means hot issues will receive long-term attention.

¹Code is available at <https://github.com/h1o2n3/ESSEN>

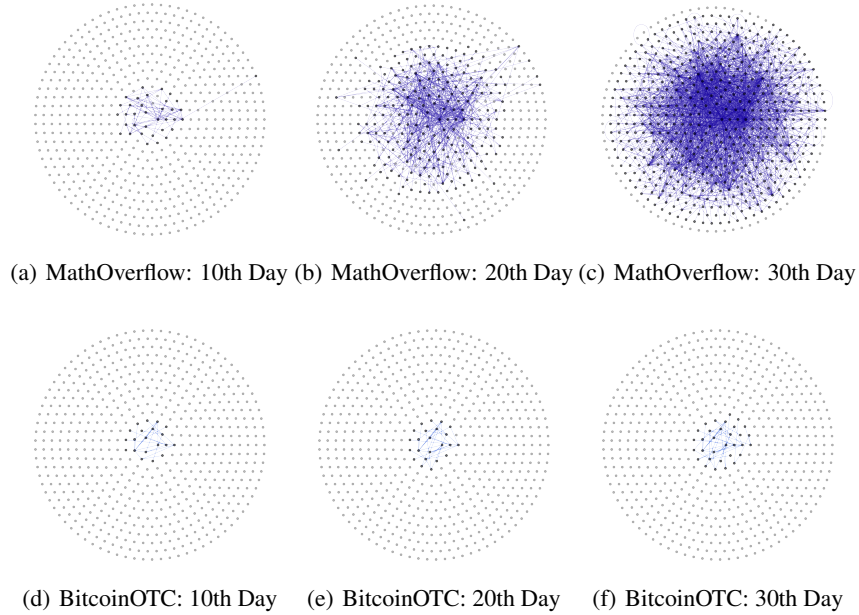


Figure 1: Network snapshots of the MathOverflow website and BitcoinOTC trading platform on the 10th, 20th, and 30th day. The black nodes represent the users who have connections, and the grey nodes represent the users with no edges prior to the snapshot time. The snapshots illustrate that temporal networks have different evolutionary states at different stages.

36 Instead, in the BitcoinOTC network, early active users may quickly become silent. The phenomenon
 37 requires algorithms that can perform extensive and effective recognition of diverse evolutionary states.
 38 (2) As time passes, temporal networks tend to accumulate more nodes and edges, resulting in an
 39 increasing number of possible connections and a rapidly growing neighborhood for each node. This
 40 growth in the neighborhood can lead to significant computational challenges when analyzing and
 41 modeling evolving patterns. Besides, many connections can quickly make structure recognition
 42 computationally infeasible in large and complex networks, especially the methods based on the
 43 anonymous walk in recent years[24; 6; 20]. The time complexity is tightly related to the length and
 44 number of paths, so it is challenging to balance time consumption and effectiveness.

45 To overcome these shortcomings, we aim to capture the evolution states using a thermodynamic
 46 entropy view. Thermodynamic network entropy is a macroscopic representation of network structures
 47 widely used to characterize the salient features of static and dynamic network systems in biology,
 48 physics, and social sciences. One of the most sophisticated studies involves the von Neumann entropy,
 49 which has been successfully used to describe the structural properties of random, small-world, and
 50 scale-free networks [1; 2]. Unfortunately, computing the required network entropies on the temporal
 51 network can be computationally burdensome due to spectral decomposition. Hence, we expand
 52 the approximate von Neumann entropy into the temporal network. Compared with other graph
 53 entropy, approximating von Neumann entropy with low time complexity can better adapt to the
 54 constantly evolving complex temporal networks. Moreover, we compute the important approximate
 55 thermodynamic quantity temperature for the temporal network. Measuring the thermodynamic
 56 temperature difference and the von Neumann entropy will provide a better understanding of the
 57 network’s evolving state at any time.

58 On this basis, we propose a novel framework named ESSEN, an **E**volution **S**tate**S** aware**E** Network.
 59 ESSEN encodes node embeddings with evolution information by utilizing two proposed techniques:
 60 von Neumann entropy aware attention mechanism and virtual evolution node representation learning.
 61 In addition, ESSEN employs a unique decoder mixture of thermodynamic experts (MoTE) for
 62 decoding. Specifically, we project the global network’s von Neumann entropy into each edge. The
 63 proposed von Neumann entropy aware attention mechanism aggregates the neighborhood in the virtual
 64 evolution graph and the original graph based on the von Neumann edge entropy. The virtual evolution
 65 graph is defined as supposing the node pair’s test connection will truly happen at the specified test time
 66 future. The MoTE decoder evaluates the evolutionary state based on the thermodynamic temperature
 67 difference and von Neumann entropy in two graph views and provides a comprehensive result from

68 multiple experts. The decoder helps to recognize the network under various evolution states adaptively.
 69 Our framework is evaluated on transductive link prediction, inductive link prediction, and dynamic
 70 node classification tasks. The experimental results demonstrate our method’s effectiveness compared
 71 to various state-of-the-art baselines. The overall contributions of our work are summarized as follows:

- 72 • To our best knowledge, we are the first to utilize the von Neumann entropy in temporal network
 73 representation learning. We provide a method to expand the approximate von Neumann Entropy
 74 and approximate thermodynamic temperature difference to temporal networks.
- 75 • We propose a novel framework, namely ESSEN. The model introduces a new perspective to encode
 76 evolution-aware node representations using the von Neumann entropy aware attention mechanism
 77 and virtual evolution node representation learning. Furthermore, the model uses a novel decoder
 78 MoTE that adaptively recognizes temporal network evolution states.
- 79 • We evaluate our framework on link prediction tasks with transductive and inductive settings.
 80 The results show the effectiveness of our proposed method compared to various state-of-the-art
 81 baselines.

82 2 Related Work

83 **Temporal Network Representation Learning.** Network representation learning is often used to
 84 transform large networks into lower-dimensional vectors. For instance, CTDNE [15] learns node
 85 embedding from a continuous-time dynamic network instead of a sequence of snapshots. Besides,
 86 JODIE [10] uses two recurrent neural networks (RNNs) to learn trajectories of users and items and
 87 updates the embedding when interaction occurs. TGAT [25] utilizes a self-attention mechanism and
 88 presents an encoding method to learn inductively. CAW [24] and NeuralTWs [6] learn temporal
 89 structure using random walk. Specifically, CAW proposes a new anonymization strategy, and
 90 NeuralTWs considers structural and tree traversal properties. TDLG[4] aims to model the edges
 91 in temporal networks directly instead of calculating from node embedding. However, it remains
 92 challenging to model global evolution under acceptable time complexity.

93 **Von Neumann Entropy of Static Graph.** The von Neumann entropy can be computed in the static
 94 graph using a quantum analogy[16]. According to this analogy, the Laplacian matrix [17] of a graph
 95 is interpreted as the density matrix [23] of an equivalent quantum system whose information content
 96 is given by the von Neumann entropy. The von Neumann entropy can be computed in the static graph
 97 as follows:

$$S_{VN} = - \sum_{i=1}^{|V|} \frac{\lambda_i}{|V|} \log \frac{\lambda_i}{|V|}, \quad (1)$$

98 where $\lambda_1, \dots, \lambda_{|V|}$ are the eigenvalues of Laplacian matrix. This form of von Neumann entropy is
 99 effective for network characterization. The thermodynamics entropy could model the structure and
 100 complexity of a graph, where the von Neumann graph entropy[3; 16; 17] is often used to describe the
 101 statistical state of a network system. De Domenico et al.[5] use von Neumann graph entropy for the
 102 structural reduction in multiplex networks. Li et al.[11] study convergence through von Neumann
 103 entropy for network-ensemble comparison. Liu et al.[13] apply von Neumann graph entropy to study
 104 universal patterns of the dynamic genome. Besides, Wang[23] calculates the approximation of von
 105 Neumann graph entropy with node degrees to model the network evolution. However, applying von
 106 Neumann entropy to represent temporal structure is still scarce. To our best knowledge, there is
 107 almost no work using von Neumann entropy to characterize the temporal graph.

108 3 Preliminaries

109 **Definition 1 Temporal Network.** Formally, the temporal network can be denoted as $G = (V, E, T)$,
 110 where V represents the set of nodes, $E \subseteq V \times V$ represents the set of links, and T represents the
 111 set of timestamps. Each link (u, v, t) signifies a connection between node u and node v at time t .
 112 The temporal network evolves over time, with links appearing at different timestamps. The temporal
 113 networks can also include attributes associated with nodes or links, providing further information
 114 about the entities or their interactions at specific timestamps.

115 **Definition 2 Dynamic Link Prediction.** In a temporal network $G = (V, E, T)$, the dynamic link
 116 prediction task aims to predict the presence or absence of a link at a future timestamp based on the

117 observed network evolution history. Given a time window $T_w \subseteq T$, which contains the observed link
 118 data, denoted as $E_{T_w} \subseteq E$, the goal is to learn a function $f : (V, E_{T_w}, T_w) \rightarrow \{0, 1\}$ that assigns
 119 a probability score to the existence of a link (u, v) at the future timestamp t . Mathematically, the
 120 function f can be defined as:

$$f(u, v, t) = P(u, v|t, E_{T_w}), \quad (2)$$

121 where $P((u, v)|t, E_{T_w})$ represents the probability of the link (u, v) being present at the future
 122 timestamp t given the observed network and the link data E_{T_w} within the time window T_w .

123 **Definition 3 Evolution States.** Evolution states denote the specific arrangements of nodes and edges
 124 at specific time moments. These states can be characterized by network topology, reflecting the
 125 evolving nature of the network over time. For example, social networks at specific evolutionary
 126 states will generate the clustering and formation of tightly-knit groups or communities over time
 127 by triadic closure theory [29]. The theory is formally defined as $\exists u, v, w, w' \in V : (u, v), (v, w) \in$
 128 $E_{T_w}, (u, w), (u, w'), (v, w') \notin E_{T_w} \mapsto P(u, w|E_{T_w}) > P(u, w'|E_{T_w})$. Therefore, analyzing evolu-
 129 tion states helps in understanding the temporal behavior of the network, identifying recurring patterns,
 130 predicting future states, and studying the impact of temporal dynamics on network properties and
 131 phenomena. In this paper, we aim to capture evolution states in a thermodynamic entropy view.

132 4 The Proposed Method

133 4.1 Evolution State Estimation

134 **Von Neumann Entropy in Temporal Network.** The von Neumann entropy can be computed in
 135 the static graph by Eq. 1. However, the application to temporal networks has two challenges: (1)
 136 The dynamic nature of the temporal network. Unlike static networks, where the structure remains
 137 constant, temporal networks capture evolving relationships and interactions. This dynamic nature
 138 introduces challenges in analyzing and modeling the network’s behavior, as the network’s topology
 139 and connectivity patterns may vary at different time points. (2) The expensive time complexity of
 140 computing the Laplacian eigenvalues. In Eq. 1, computing the eigenvalues of the Laplacian matrix is
 141 a computationally intensive task and the time complexity grows with the size of the network. The
 142 time cost is cubic in the number of nodes. In temporal networks, where the network structure changes
 143 over time, repeatedly calculating the Laplacian eigenvalues can become prohibitively expensive and
 144 time-consuming.

145 To solve these challenges, we must simplify the network and efficiently approximate thermodynamic
 146 quantities. **First**, we select a specific time interval from the temporal network and aggregate edge
 147 weights or frequencies, where the number of occurrences within the chosen time frame determines
 148 the strength of an edge. Following this process, the temporal network can be projected to the
 149 time-independent 2-D plane, which provides a simplified representation of the underlying network
 150 structure at a specific time. **Moreover**, inspired by [27], we use the approximate expression for
 151 the von Neumann entropy and reduce the computation to quadratic in the number of nodes. The
 152 approximate von Neumann entropy is

$$S_{VN}(G_t) = 1 - \frac{1}{|V|} - \frac{1}{|V|^2} \sum_{(u,v) \in E} \frac{1}{d_u d_v}, \quad (3)$$

153 where V is the node set of the temporal network, and d_u, d_v are the degree of node u and v at time t .
 154 This approximation allows the von Neumann entropy to be computed without explicitly solving the
 155 eigensystem for the normalized Laplacian. The proof of the approximate von Neumann entropy is
 156 presented in Appendix A. Thus, the von Neumann entropy can be computed in quadratic time using
 157 the node degrees for pairs of nodes connected by edges.

158 **Thermodynamic Temperature Differences.** In thermodynamics, a thermodynamic state of a system
 159 can be fully described by an appropriate set of principal parameters known as thermodynamic
 160 variables. Due to the dynamic nature of the temporal network, it is not sufficient to simply evaluate
 161 the evolution states for two moments using the von Neumann entropy. Thus, we introduce the
 162 thermodynamic temperature difference, defined as the rate of energy change with entropy between
 163 two networks, to complement the description of the network dynamics system. The expression which
 164 subject to the condition that the volume and number of particles are constant is shown as follows:

$$\mathcal{T}(G_1, G_2) = \frac{de}{dS} = \frac{e(G_1) - e(G_2)}{S(G_1) - S(G_2)}, \quad (4)$$

165 where $S(G_1)$ is the graph entropy on the graph G_1 and $e(G_1)$ is the graph average energy. The subject
 166 can be applied to temporal networks since the networks do not change significantly in node number
 167 during evolution. The thermodynamic temperature difference can bridge the graphs of two moments.
 168 More importantly, the thermodynamic temperature difference can also be approximated when we
 169 project the temporal network as a weighted graph, like in the computing process of von Neumann
 170 entropy. The approximate computation method uses low-order Taylor series that can be computed
 171 using the traces of powers of the normalized Laplacian matrix, avoiding explicit computation of the
 172 normalized Laplacian spectrum [26]. The detailed derivation process is in Appendix A. In summary,
 173 the temperature difference between the two networks can be approximated as

$$\mathcal{T}(G_1, G_2) = -\frac{2}{k} + \frac{2}{3k} \cdot \frac{\mathcal{K}(G_1) - \mathcal{K}(G_2)}{\mathcal{J}(G_1) - \mathcal{J}(G_2)}, \quad (5)$$

174 where

$$\mathcal{J}(G) = \sum_{u,v \in V} \frac{A_{uv}}{d_u d_v}, \quad (6)$$

175

$$\mathcal{K}(G) = \sum_{u,v,w \in V} \frac{A_{uv} A_{vw} A_{wu}}{d_u d_v d_w}, \quad (7)$$

176 k is the Boltzmann constant, and A is the adjacency matrix of the network. Especially we denote
 177 G'_{uv} as the graph G adds a new connection between u and v , the computation of $\mathcal{T}(G, G'_{uv})$ can
 178 be reduced as quadratic in the number of nodes. Because the expressions $\mathcal{J}(G'_{uv}) - \mathcal{J}(G)$ and
 179 $\mathcal{K}(G'_{uv}) - \mathcal{K}(G)$ can be rewritten as

$$\begin{aligned} \mathcal{J}(G'_{uv}) - \mathcal{J}(G) &= \sum_{i \in V} \frac{A_{iv}}{d_i d_v (d_v + 1)} + \frac{A_{iu}}{d_i d_u (d_u + 1)}, \\ \mathcal{K}(G'_{uv}) - \mathcal{K}(G) &= \sum_{i,j \in V} \frac{A_{iv} A_{jv} A_{ij}}{d_i d_j d_v (d_v + 1)} + \frac{A_{iu} A_{ju} A_{ij}}{d_i d_j d_u (d_u + 1)} + \sum_{i \in V} \frac{A_{iv} A_{iu} A_{uv}}{d_i d_u d_v (d_u + 1)(d_v + 1)}. \end{aligned} \quad (8)$$

180 In summary, by simplifying the network representation and using efficient approximations, the
 181 von Neumann entropy and thermodynamic temperature difference can be computed effectively in
 182 temporal networks. These measures provide insights into the evolving nature of the network and
 183 enable the estimation of its evolution state.

184 4.2 Evolution States Aware Graph Encoder

185 **Von Neumann Entropy Aware Attention Mechanism.** In graph encoding, we utilize the von
 186 Neumann entropy to explore a more diverse and balanced distribution of attention weights with
 187 the attention mechanism in the input neighborhood. This strategy helps the model learn network
 188 evolution states adaptively. According to Eq. 3, the global network entropy is a sum of contributions
 189 from individual edges. Thus, we decompose the global network entropy into components residing on
 190 the individual edges, so the von Neumann entropy of the edge connecting nodes u and v is

$$S_{VN}^{uv}(G_t) = \frac{1}{|E|} - \frac{1}{|V||E|} - \frac{1}{|E||V|^2} \frac{1}{d_u d_v}, \quad (9)$$

191 To better encode entropy features into attention layers, we incorporate the edge expression of von
 192 Neumann entropy via a bias term to the attention module[22]. Moreover, we use a time position
 193 encoding module[25] to supplement the continuous time information of edges simplified in the von
 194 Neumann entropy. Concretely, given a target node u at time t , the attention weight $\alpha_v^{(l)}$ from the
 195 neighbor node v on the l^{th} layer as

$$\alpha_v^{(l)} = \frac{Q_u^{(l)} \left(K_v^{(l)} \right)^T}{\sqrt{d}} + S_{VN}^{uv}(G_t), \quad (10)$$

196

$$Q_u^{(l)} = (h_u^{(l-1)} \| e_0 \| \phi(0)) W_Q, \quad (11)$$

197

$$K_v^{(l)} = M_{v,t}^{(l)} W_K, \quad (12)$$

198

$$M_{v,t}^{(l)} = \left(h_v^{(l-1)} \| e_{uv,t} \| \phi(t_q - t) \right) W_M, \quad (13)$$

199 where d is the dimension of the node representation and “ $\|$ ” is the concatenation operation. $W_K \in \mathbb{R}^{(d+d_t+d_e) \times d}$ and $W_Q \in \mathbb{R}^{(d+d_t+d_e) \times d}$ are the projection matrices to obtain the query matrices and
 200 key matrices. e_0 is an all-zero vector to keep the same dimension as K and V , and $\phi(\ast)$ is the
 201 generic time position encoding module from [25], which encodes the difference between the edge’s
 202 timestamp and query timestamp. $M_{v,t}^{(l)}$ is the message representation at time t from node v to u ,
 203 where $h_v^{(l-1)}$ is node v ’s hidden representation on the $(l-1)^{th}$ layer, $e_{uv,t} \in \mathbb{R}^{d_e}$ is the edge feature,
 204 and t_q is the query time.
 205

206 Next, the model combines values with the attention weight aware of generating hidden representation
 207 $z_u^{(l)}(t)$ for node u . Finally, an MLP is used to combine the node representation of the previous layer
 208 with the neighborhood information:

$$h_u^{(l)} = MLP(h_u^{(l-1)} \| z_u^{(l)}(t)), \quad (14)$$

209

$$z_u^{(l)}(t) = \sum_{v \in \mathcal{N}_u} \text{softmax}_v(\alpha_v(t)) V_v(t), \quad (15)$$

210

$$V_v^{(l)} = M_{uv,t}^{(l)} W_V, \quad (16)$$

211 where $V_v^{(l)}$ is the value vector of neighbor node v , and \mathcal{N}_u is a neighbor node set that connects with
 212 node u before time t .

213 **Virtual Evolution Node Representation Learning.** Temporal net-
 214 works follow evolution laws in the progress of time. The emergence
 215 of nodes and edges is often predictive, i.e., future network states
 216 can be predicted by past states and evolutionary laws. The network
 217 evolution state representation learning utilizes historical evolution
 218 information and the future virtual evolution graph to generate node
 219 representations. Specifically, the dynamic link prediction task aims
 220 to predict the probability of the link between two nodes appearing
 221 at a future moment. We suppose the link has been generated at the
 222 query moment and further construct the virtual evolution graph be-
 223 longing to the query node pair on this suppose. For example, given a
 224 node pair (u, v) and the query time t , there is a virtual bridge at time
 225 t that connects the node u and v in the virtual evolution graph G'_{uv} . The approach makes the two
 226 node’s neighborhoods interconnected. We denote h'_u and h'_v as the virtual future node embedding of
 227 u and v . Our framework will further measure the evolution differences through the decoding process.

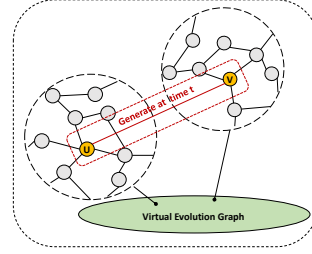


Figure 2: Virtual evolution graph of u, v at time t .

228 4.3 Mixture of Thermodynamic Experts Decoder

229 **Expert Assessment Features.** We use the von Neuman entropy of the original graph, the von Neuman
 230 entropy of the virtual evolution graph, and the thermodynamic temperature difference between both
 231 networks to combine a unique vector as expert assessment features. The vector represents the
 232 network’s evolution states in the 3-D thermodynamic space, which is made up of current time and
 233 future time’s von Neumann entropy and the thermodynamic temperature. We use Eq. 5 to approximate
 234 the thermodynamic temperature difference and Eq. 3 to compute the von Neumann graph entropy for
 235 the original and virtual evolution graphs. Furthermore, to control evolution-aware ranges, which is
 236 important for large temporal networks, we compute these approximate thermodynamic quantities in
 237 the node’s neighborhood and set the sampled neighborhood size N .

238 **Decoding Process.** The mixture of thermodynamic experts decoder dynamically selects the appro-
 239 priate thermodynamic expert model based on the input expert assessment feature vectors. For each
 240 expert, we use a two-layers MLP model to represent. Then the MoTE decoder combines the output
 241 embedding of each expert model using respective expert weights to produce the final target score as
 242 follows:

$$\text{score}(u, v, t) = \sum_{i=1}^M \sigma(W_i(h_u, h_v, h'_v - h_v, h'_u - h_u)) \pi_i, \quad (17)$$

Table 1: Performance of AUC(%) for link prediction. The best results in each column are highlighted in bold font and the second-best results are underlined. We report the AP results in Appendix B.

Task	Methods	MathOverflow	BitcoinAlpha	BitcoinOTC	Wikipedia
Transductive	JODIE	86.07 ±0.48	91.14 ±0.18	92.29 ±0.11	94.62 ±0.50
	DyRep	80.77 ±0.65	79.39 ±3.17	79.21 ±4.10	94.59 ±0.20
	TGN	80.47 ±3.24	86.71 ±1.00	86.78 ±2.29	98.46 ±0.10
	TGAT	71.80 ±0.91	78.99 ±0.50	79.53 ±0.67	95.34 ±0.10
	CAW	53.82 ±0.28	64.70 ±0.93	73.95 ±1.22	<u>98.96 ±0.10</u>
	TDLG	84.02 ±0.16	92.83 ±0.22	93.48 ±0.22	88.93 ±0.09
	P-INT	54.09 ±3.24	88.11 ±0.60	91.26 ±0.69	98.78 ±0.10
	NeurTWs	<u>92.56 ±0.51</u>	<u>93.95 ±0.41</u>	<u>95.75 ±0.01</u>	94.54 ±0.87
	ESSEN	98.60 ±0.40	99.10 ±0.16	98.88 ±0.42	99.03 ±0.33
Inductive	JODIE	67.06 ±0.42	74.47 ±0.16	76.21 ±0.47	93.11 ±0.40
	DyRep	63.50 ±0.66	66.27 ±0.73	65.09 ±0.86	92.05 ±0.30
	TGN	64.50 ±1.17	69.36 ±0.94	76.52 ±1.25	97.81 ±0.10
	TGAT	60.02 ±0.75	66.42 ±1.17	66.62 ±1.99	93.99 ±0.30
	CAW	57.67 ±0.33	64.38 ±1.01	72.99 ±0.46	<u>98.75 ±0.14</u>
	TDLG	74.31 ±1.58	83.85 ±1.65	85.22 ±3.89	45.77 ±3.06
	P-INT	50.16 ±1.46	77.88 ±0.93	83.76 ±0.98	98.38 ±0.40
	NeurTWs	<u>91.83 ±0.13</u>	<u>94.20 ±0.26</u>	<u>96.08 ±0.38</u>	94.63 ±0.47
	ESSEN	98.33 ±0.28	98.07 ±0.64	98.67 ±0.31	98.80 ±0.10

243

$$\pi_i = \text{softmax}_i((\mathcal{T}(G, G'_{uv}) \| S_{VN}(G)) \| S_{VN}(G'_{uv})) W_\pi), \quad (18)$$

244 where M is the total number of experts, π_i is the mixing coefficient of expert i . $W_i \in \mathbb{R}^{4d \times 1}$ is the
 245 weight matrices for expert i . And $W_\pi \in \mathbb{R}^{3 \times M}$ is the weight matrix of the gate unit. h_v and h'_v
 246 are the embeddings of node v in the original graph and virtual evolution graph generated by the encoder.

247 4.4 Optimization

248 During training, we evaluated the convergence behavior of our model by monitoring the training and
 249 validation loss, ensuring that the model was not underfitting or overfitting. The loss function is shown
 250 as follows:

$$\ell = \sum_{(v_i, v_j, t_{ij}) \in \mathcal{E}} -\log P(v_i, v_j | t_{ij}) - \mathcal{Q} \cdot \mathbf{E}_{\tilde{v} \sim P(\tilde{v})} \log P(v_i, \tilde{v} | t_{ij}), \quad (19)$$

251 where (v_i, v_j, t_{ij}) is the observed edge on the temporal network, \mathcal{Q} denotes the number of negative
 252 samples, and $P(\tilde{v})$ is the negative sampling distribution over the node space \mathbf{E} .

253 4.5 Computational Complexity Analysis

254 This section aims to highlight the efficiency of our approach in calculating approximate thermo-
 255 dynamic quantities of temporal networks. Based on Eq.3, Eq. 5, and Eq. 8, the time complexity
 256 of computing approximate von Neumann entropy and the approximate temperature difference is
 257 $O(|V|^2)$, where $|V|$ is the number of nodes in the network. Moreover, we compute the approximate
 258 thermodynamic quantities in the neighborhood for the large networks and set the sampled neighbor-
 259 hood size N . In this setting, the computational complexity can be reduced to $O(N^2)$, where N is
 260 the settable number. Therefore, the time complexity demonstrates scalability and feasibility for our
 261 method to operate in moderate or large networks. The controllable time complexity ensures efficient
 262 computation.

263 5 Experiments

264 5.1 Experimental Setup

265 **Datasets.** The temporal network datasets of our
 266 experiment are divided into three types: (a) QA:
 267 The “answers to questions” dataset of MathOver-
 268 flow. (b) Bitcoin trading data: BitcoinAlpha
 269 Dataset and BitcoinOTC Dataset [9; 8]. (c) So-
 270 cial networks: Wikipedia Dataset[10]. Table 2
 271 reports more details about these datasets.

Dataset	Nodes	Edges	Timespan
MathOverflow	21,688	107,581	2350 days
BitcoinOTC	5,881	35,592	1903 days
BitcoinAlpha	3,783	24,186	1901 days
Wikipedia	9,227	157,474	30 days

272 **Baselines.** In addition to reporting our ESSEN method’s performance, we report results for several
 273 popular dynamic methods: a) JODIE [10]; b) DyRep [21]; c) TGAT [25]; d) TGN [19]; e) CAW [24];
 274 f) TDLG[4]; g) P-INT[20]; and h) NeurTWs[6]. We report more details about baselines in Appendix
 275 C.

276 **Link Prediction Task Settings.** We evaluate our model on the link prediction task with two significant
 277 settings:

- 278 • **Transductive Setting.** The model under the transductive setting is trained on available nodes
 279 and their connections to predict links between these nodes in the future. The setting assumes
 280 the network will not add unseen nodes in the future test time. It mainly evaluates the model’s
 281 transductive ability.
- 282 • **Inductive Setting.** The inductive setting predicts missing links for existing nodes and potential
 283 new nodes that may be added in the future. It generalizes link prediction beyond known nodes,
 284 considering the possibility of new nodes. It learns network patterns and characteristics to make
 285 predictions applicable to both known and unknown nodes.

286 **Implementation Training Details.** For each dataset, we used the training time points $T_{tr} = 70\%$
 287 to split the dataset results in approximately 70%-15%-15% of the total edges [25]. The principal
 288 hyperparameters are set as follows: a) the number of attention heads $\mathcal{U} = \{2, 3\}$, b) the number of
 289 the GNN layers $\mathcal{L} = 2$, c) the maximum number of aggregated neighbors $n \in \{60, 80, 100\}$, d) the
 290 total number of experts in MoTE $M = \{4, 6, 8, 10\}$, and e) the dimension of the node embedding
 291 $D = 172$. We use the ADAM optimization algorithm for model training with a learning rate 1e-3
 292 and batch size of 128. All the models are implemented in PyTorch and evaluated on a single Tesla
 293 A100 GPU.

294 5.2 Results and Discussion

295 Table 1 reports the transductive and inductive link prediction task results on four datasets, demonstrat-
 296 ing our method’s state-of-the-art performance on link prediction tasks. Indeed, our model significantly
 297 outperforms all baselines on all datasets. In particular, in the MathOverflow dataset, compared with
 298 NeurTWs, the second strongest baseline, ESSEN improved the AUC(%) by 5.04% and 6.50% on
 299 average on the transductive and inductive setting. The results demonstrate that our method has a
 300 clear advantage for temporal networks. Specifically, our method performs well on both long and
 301 short evolution time networks, while the effectiveness of baseline models varies significantly. CAW
 302 and TGAT have enormous performance gaps between MathOverflow and Wikipedia in all tasks.
 303 It indicates that our framework represents the network with ever-changing evolution states better.
 304 The superiority can be attributed to our von Neumann entropy aware mechanism, virtual evolution
 305 node representation learning, and MoTE decoder. In addition, our method is effective under both
 306 transductive and inductive settings. On the contrary, the baseline method JODIE cannot predict
 307 interactions well between unseen nodes because it pays more attention to node identities rather than
 308 the evolution states of temporal networks.

309 5.3 Ablation Study and Time Comparison

310 **Ablation Study.** To validate the effectiveness of the elements
 311 comprising ESSEN, we conduct a series of ablation studies
 312 and report the AUC results. We investigated the proposed mod-
 313 ules with three ablated models on the Bitcoin-alpha dataset:
 314 a)ESSEN- E , the model removes the von Neumann edge en-
 315 tropy bias in the attention mechanism of ESSEN. b)ESSEN- V ,
 316 the model removes virtual evolution node representation and

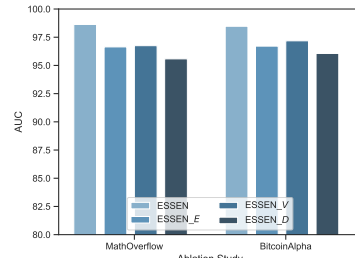


Figure 3: Ablation Study

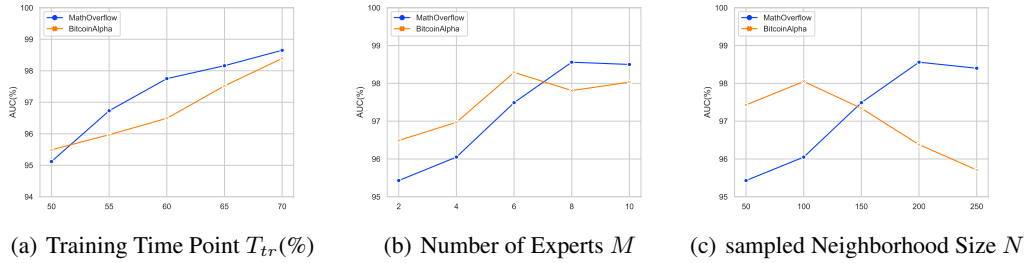


Figure 5: Study on important settings. We report the results of the inductive link prediction.

317 only uses the node embeddings of the original graph for decoding. c) ESSEN- D , the model replaces
 318 the MoTE decoder with a simple MLP decoder. In Fig. 3, we can see the performance degradation
 319 without considering the von Neumann entropy information of edges, demonstrating the effectiveness
 320 of the proposed von Neumann entropy aware attention mechanism. Disabling the virtual evolution
 321 node representation also hurts performance. Furthermore, when the MoTE decoder is removed,
 322 BitcoinOTC and BitcoinAlpha exhibit more severe performance drops, demonstrating that the MoTE
 323 decoder excels on temporal networks with a long time span and more evolution states.

324 **Time Comparison.** Fig.4 compares the training times of ESSEN
 325 against the second-strongest baseline NTW. For fairness, we use the
 326 same batch size for both models and experiment in the same environ-
 327 nment. Note that the running time of ESSEN is down quickly because
 328 the approximate thermodynamic quantities have been computed at
 329 the first epoch and use cache after that. If we pre-computed thermo-
 330 dynamic quantities for the model, ESSEN would run considerably
 331 faster than NTW.

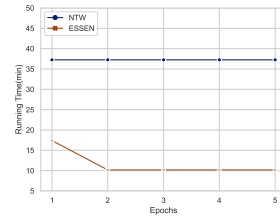


Figure 4: Time Comparison.

332 5.4 Parametric Sensitivity

333 we investigate the sensitivity of our ESSEN to various parameters and evaluate their impact on
 334 the model’s performance. In Fig. 5, We report the results and have the following observations: a)
 335 Through the exploration of different training time points, our model keeps excellent performance,
 336 even if the number of samples in the training set is reduced since the training time shift. Especially,
 337 lowering the training time point means increasing the testing of more samples in the future. It clearly
 338 shows the robustness of ESSEN for complex evolutionary states. b) Regarding the number of experts
 339 M , there are sweet spots in both datasets. This finding indicates that different datasets exhibit a
 340 preference for specific numbers of experts in the MoTE decoder, which can be attributed to the
 341 varying complexity of evolutionary states in the temporal network. c) We observe a strong correlation
 342 between the evolution-aware size N and the node number of the temporal network. For instance,
 343 the MathOverflow with more number nodes has better performance with the large evolution-aware
 344 neighborhood. On the contrary, it negatively impacts the performance of BitcoinAlpha when N is
 345 higher than 100.

346 6 Conclusion

347 In this paper, we propose ESSEN, an Evolution StateS awarE Network for recognizing and analyzing
 348 the evolution states on temporal networks. We addressed the limitations of existing methods in
 349 capturing the time-varying nature of network structures, especially in complex evolving states. Our
 350 framework incorporates a von Neumann entropy aware attention mechanism and network evolution
 351 state contrastive learning in the graph encoding. The decoding stage utilizes a unique decoder called
 352 Mixture of Thermodynamic Experts (MoTE). We evaluated ESSEN on link prediction tasks in
 353 transductive and inductive settings and compared it to state-of-the-art baselines. The experimental
 354 results demonstrate the effectiveness of our proposed method in capturing temporal dynamics and
 355 outperforming existing approaches. Our work contributes to advancing the field of temporal network
 356 analysis and opens up possibilities for future research in other domains and additional network
 357 dynamics. In the future, we will focus on improving ESSEN’s efficiency and scalability, allowing it
 358 to handle larger datasets and real-time analysis.

References

- 359
- 360 [1] Alstott, J., Pajevic, S., Bullmore, E., Plenz, D.: Opening bottlenecks on weighted networks by local
361 adaptation to cascade failures. *Journal of Complex Networks* **3**(4), 552–565 (2015)
- 362 [2] Anand, K., Krioukov, D., Bianconi, G.: Entropy distribution and condensation in random networks with a
363 given degree distribution. *Physical Review E* **89**(6), 062807 (2014)
- 364 [3] Braunstein, S.L., Ghosh, S., Severini, S.: The laplacian of a graph as a density matrix: a basic combinatorial
365 approach to separability of mixed states. *Annals of Combinatorics* **10**(3), 291–317 (2006)
- 366 [4] Chanpuriya, S., Rossi, R.A., Kim, S., Yu, T., Hoffswell, J., Lipka, N., Guo, S., Musco, C.: Direct
367 embedding of temporal network edges via time-decayed line graphs. In: *ICLR (2022)*
- 368 [5] De Domenico, M., Nicosia, V., Arenas, A., Latora, V.: Structural reducibility of multilayer networks.
369 *Nature communications* **6**(1), 1–9 (2015)
- 370 [6] Jin, M., Li, Y.F., Pan, S.: Neural temporal walks: Motif-aware representation learning on continuous-time
371 dynamic graphs. In: *NeurIPS (2022)*
- 372 [7] Kipf, T.N., Welling, M.: Semi-supervised classification with graph convolutional networks. In: *ICLR*
373 (2016)
- 374 [8] Kumar, S., Hooi, B., Makhija, D., Kumar, M., Faloutsos, C., Subrahmanian, V.: Rev2: Fraudulent user
375 prediction in rating platforms. In: *WSDM*. pp. 333–341. *ACM* (2018)
- 376 [9] Kumar, S., Spezzano, F., Subrahmanian, V., Faloutsos, C.: Edge weight prediction in weighted signed
377 networks. In: *ICDM*. pp. 221–230. *IEEE* (2016)
- 378 [10] Kumar, S., Zhang, X., Leskovec, J.: Predicting dynamic embedding trajectory in temporal interaction
379 networks. In: *SIGKDD*. *ACM* (2019)
- 380 [11] Li, Z., Mucha, P.J., Taylor, D.: Network-ensemble comparisons with stochastic rewiring and von neumann
381 entropy. *SIAM journal on applied mathematics* **78**(2), 897–920 (2018)
- 382 [12] Liben-Nowell, D., Kleinberg, J.: The link-prediction problem for social networks. *Journal of the American*
383 *society for information science and technology* **58**(7), 1019–1031 (2007)
- 384 [13] Liu, S., Chen, P.Y., Hero, A., Rajapakse, I.: Dynamic network analysis of the 4d nucleome. *bioRxiv* p.
385 268318 (2018)
- 386 [14] Monti, F., Boscaini, D., Masci, J., Rodola, E., Svoboda, J., Bronstein, M.M.: Geometric deep learning on
387 graphs and manifolds using mixture model cnns. In: *CVPR*. pp. 5115–5124 (2017)
- 388 [15] Nguyen, G.H., Lee, J.B., Rossi, R.A., Ahmed, N.K., Koh, E., Kim, S.: Continuous-time dynamic network
389 embeddings. In: *WWW*. pp. 969–976 (2018)
- 390 [16] Passerini, F., Severini, S.: The von neumann entropy of networks. Available at SSRN 1382662 (2008)
- 391 [17] Passerini, F., Severini, S.: Quantifying complexity in networks: the von neumann entropy. *International*
392 *Journal of Agent Technologies and Systems (IJATS)* **1**(4), 58–67 (2009)
- 393 [18] Ren, H., Leskovec, J.: Beta embeddings for multi-hop logical reasoning in knowledge graphs. In: *NeurIPS*.
394 vol. 33, pp. 19716–19726 (2020)
- 395 [19] Rossi, E., Chamberlain, B., Frasca, F., Eynard, D., Monti, F., Bronstein, M.: Temporal graph networks for
396 deep learning on dynamic graphs. In: *ICLR (2020)*
- 397 [20] Souza, A., Mesquita, D., Kaski, S., Garg, V.: Provably expressive temporal graph networks. *Advances in*
398 *Neural Information Processing Systems* **35**, 32257–32269 (2022)
- 399 [21] Trivedi, R., Farajtabar, M., Biswal, P., Zha, H.: Dyrep: Learning representations over dynamic graphs. In:
400 *ICLR (2019)*
- 401 [22] Vaswani, A., Shazeer, N., Parmar, N., Uszkoreit, J., Jones, L., Gomez, A.N., Kaiser, Ł., Polosukhin, I.:
402 Attention is all you need. *Advances in neural information processing systems* **30** (2017)
- 403 [23] Wang, J.: *Statistical Mechanics for Network Structure and Evolution*. Ph.D. thesis, University of York
404 (2018)

- 405 [24] Wang, Y., Chang, Y.Y., Liu, Y., Leskovec, J., Li, P.: Inductive representation learning in temporal networks
406 via causal anonymous walks. In: ICLR (2021)
- 407 [25] Xu, D., Ruan, C., Korpeoglu, E., Kumar, S., Achan, K.: Inductive representation learning on temporal
408 graphs. In: ICLR (2020)
- 409 [26] Ye, C., Comin, C.H., Peron, T.K.D., Silva, F.N., Rodrigues, F.A., Costa, L.d.F., Torsello, A., Hancock,
410 E.R.: Thermodynamic characterization of networks using graph polynomials. *Physical Review E* **92**(3),
411 032810 (2015)
- 412 [27] Ye, C., Wilson, R.C., Comin, C.H., Costa, L.d.F., Hancock, E.R.: Approximate von neumann entropy for
413 directed graphs. *Physical Review E* **89**(5), 052804 (2014)
- 414 [28] Zhang, M., Chen, Y.: Link prediction based on graph neural networks. *Advances in neural information
415 processing systems* **31** (2018)
- 416 [29] Zhou, L., Yang, Y., Ren, X., Wu, F., Zhuang, Y.: Dynamic network embedding by modeling triadic closure
417 process. In: *Proceedings of the AAAI conference on artificial intelligence*. vol. 32 (2018)